Utilizing DNA for Electrocatalysis: DNA-Nickel Aggregates as Anodic Electrocatalysts for Methanol, Ethanol, Glycerol, and Glucose

Dayi Chen,* **Garett G. W. Lee, and Shelley D. Minteer**,**,z

Departments of Chemistry and Materials Science and Engineering, University of Utah, Salt Lake City, Utah 84112, USA

DNA-nickel aggregates were electrodeposited onto glassy carbon electrode surfaces and have shown electrocatalytic activity for oxidation of methanol, ethanol, glycerol, and glucose at room temperature in alkaline solutions. Bulk electrolysis oxidation products identified by ^{13}C NMR include carbonate as methanol, glycerol, and glucose's oxidation products suggesting these three fuels can be deeply oxidized by DNA-nickel aggregates and carbon-carbon bonds can be broken during the oxidation of glycerol and glucose. However, ethanol was only oxidized to acetate. The capability of deep oxidation of methanol, ethanol, glycerol and glucose under relatively moderate conditions makes DNA-nickel a candidate for fuel cell applications.

Fuel cells are high energy density, energy conversion devices, which have application for portable power.[1] To utilize the energy stored in the fuel completely and efficiently, efficient electrocatalysts are needed. Besides expensive precious metals and/or toxic rare metals,[2] nickel based catalysts can also be considered for the oxidation of alkanes,[3] alcohols, amines and carbohydrates.[4] So far, various nickel complexes, usually immobilized in polymer films, having nickel coordinated to nitrogen, oxygen or phosphorus have been developed for oxidation of short chain alcohols in alkaline media.[5–7]

Wei et al. developed a nickel catalyst for a methanol sensor in alkaline media utilizing DNA for formation of catalytic structures on electrode surfaces. DNA-nickel aggregates were electrodeposited onto a glassy carbon electrode[8] and the electrodes showed a linear amperometric response for methanol from 2.0 μM to 3 mM, showing they can catalyze the methanol oxidation. Although this catalyst was developed for a sensor, the cyclic voltammograms generated from using 0.1 M methanol in 0.1 M NaOH showed that the catalyst can tolerate much higher methanol concentrations and therefore may be suitable to other applications, including fuel cell electrocatalysis. Utilizing DNA as the immobilization matrix for nickel may provide many benefits (i.e. the three-dimensional structure of DNA could have some unexpected positive catalytic effects[9] and DNA could be used as a self-assembly template[10]). The DNA structure may also promote the catalytic activity of nickel and provide the DNA-based nickel catalysts a promising future as electrocatalysts for fuel cell applications. However, the structure/function relationship of this DNA-nickel catalyst has not been studied in Wei et al.'s study, and the catalytic specificity and degree of oxidation, which are important for fuel cell applications, have not been evaluated either.

In alkaline media, methanol can lose two electrons to produce formaldehyde, four electrons to produce formate, or six electrons to produce carbonate; but Wei et al. did not study the degree of oxidation of alcohol-based fuels, so the efficiency of the DNA-nickel aggregate for electrocatalysis is still unknown. Moreover, only methanol was tested for oxidation; but since other nickel catalysts have been reported to oxidize various fuel species, there could be more fuel options.

In our study, the morphology and the composition of the DNA-nickel aggregates have been characterized via atomic force microscopy (AFM), scanning electron microscopy (SEM) and X-ray photoelectron spectroscopy (XPS). We studied the catalytic oxidation of a variety of fuels including methanol, ethanol, glycerol, and glucose via the DNA-nickel aggregates, and identified oxidation products to show all of these fuels are deeply oxidized at room temperature in 0.1 M NaOH. This work is the first evidence of the broad use of these

DNA-nickel aggregates as oxidation catalysts, indicating the DNA-nickel aggregates can be an anodic electrocatalyst candidate for fuel cells in alkaline media.

Experimental

Electrodeposition of DNA-Nickel aggregates.— Glassy carbon (GC) electrodes were polished with 1 μm and 0.05 μm alumina (Buehler) successively and then sonicated in water and ethanol. According to Wei et al.'s procedure,[8] a 0.1 mg/mL DNA solution and a 0.5 mg/mL $NiCl_2$ solution were made and then mixed and stirred for an hour. Sodium chloride was added before electrodeposition to make an electrolyte solution containing 0.1 M NaCl. Solutions with only 0.1 mg/mL DNA, 0.5 mg/mL $NiCl_2$ and 0.1 M NaCl were also prepared for the control experiments. Electrodeposition of DNA-nickel or DNA or $NiCl_2$ onto glassy carbon electrode surfaces was performed with a CH Instruments 611C potentiostat interfaced to a PC computer at 1.8 V (vs. Ag/AgCl(1 M)) for 30 minutes. A three-electrode configuration was used throughout all the electrochemical measurements. The glassy carbon (GC) electrode (diameter 3 mm) was used as the working electrode, platinum mesh as the counter electrode, and Ag/AgCl(1M) as the reference electrode for the experiments, except in the bulk electrolysis, where a Hg/HgO (0.1M NaOH) reference electrode was used. The same electrodeposition procedure was done to glassy carbon plates for the microscopy and spectroscopy analysis.

Cyclic voltammetric experiments.— All cyclic voltammograms (CVs) were collected in the 3-electrode configuration mentioned above. In 0.1M NaOH, 0.1M sodium formate (pH 12.8–12.9), 0.1M formaldehyde (pH 12.8–12.9), 0.1M methanol (pH 12.8–12.9), 0.1M ethanol (pH 12.8–12.9), 0.025M glycerol (pH 12.8–12.9), and 0.025M glucose (pH 12.7–12.8) solutions were prepared. CVs were taken between 0.2 V and 0.8 V at 0.05 V/s at room temperature. All solutions were degassed with nitrogen and all experiments performed in triplicate.

Bulk electrolysis and product determinations.— Bulk electrolysis of 0.1 M methanol-^{13}C, 0.1 M ethanol-2-^{13}C, 0.025 M glycerol-$^{13}C3$ and 0.025 M glucose-$^{13}C6$ in 0.1 M NaOH was conducted with either a Pine Wavenow potentiostat or a CH Instruments 650A potentiostat at 0.67V vs Hg|HgO. Because glucose can be oxidized by air in the alkaline media, the bulk electrolysis of glucose was performed in an anaerobic glove box (filled with nitrogen). The bulk electrolysis was run for 72 hours in triplicate for each fuel, with samples taken at 0 hr, 1 hr, 6 hr, 24 hr, 48 hr, and 72 hr. ^{13}C spectra obtained by Varian Unity 300 MHz NMR were used to confirm the bulk electrolysis products.

*Electrochemical Society Student Member.
**Electrochemical Society Active Member.
zE-mail: minteer@chem.utah.edu

Equal volume of D$_2$O was added to each sample and 1800 scans were taken.[11]

Results and Discussion

Surface morphologies were characterized with SEM and AFM. The DNA aggregates measured in Figure 1a are a little shorter and wider than the natural DNA strands purchased. However, the DNA-nickel aggregates (Figure 1b) are much larger aggregates than the DNA aggregates (Figure 1a), probably due to the easier crosslinking of DNA strands via nickel ion bridges[12] and the shielding of negative charges of phosphate groups, which reduces the repulsion between the DNA molecules.[13] The EDS analysis[11] of the DNA-nickel aggregates shows there are DNA and nickel present with a small amount of NaCl and KCl (Atomic%: C 59.46, N 12.76, O 24.99, P 1.64, Ni 0.48, Na 0.23, Cl 0.24, K 0.20). Also, the SEM images in Figure 1b show the aggregates have porous structures, providing an open framework for fuel transport.

For AFM characterization, the bare glassy carbon plate shown in Figure 1c has a 0.577 nm root-mean-square roughness for a 1 μm × 1 μm surface area, so the glassy carbon plate is flat enough for use as an AFM substrate. Since the DNA aggregates and DNA-nickel aggregates were electrodeposited in NaCl solution, a control experiment was performed where GC plates were submerged in 0.1 M NaCl followed by application of 1.8 V. The representative micrograph for this control is shown in Figure 1d, which had a roughness of 1.26 nm (effectively flat). Both DNA (Figure 1e) and DNA-nickel aggregates (Figure 1g) samples contain small particles overlapping each other instead of the long strands usually observed on hydrophilic mica surface,[14,15] while the nickel only sample (Figure 1f) has even smaller particles with a roughness of only 1.34 nm. Section analysis, as shown in Figure S1 of the Supporting Information,[11] indicates most particles in the nickel sample have the height of 1–2 nm, while in the DNA sample most particles have the height of 5–7 nm, with some large particles (10–15 nm) and some smaller particles of 2–3 nm. In the DNA-nickel sample, most particles have a height of 10–15 nm,
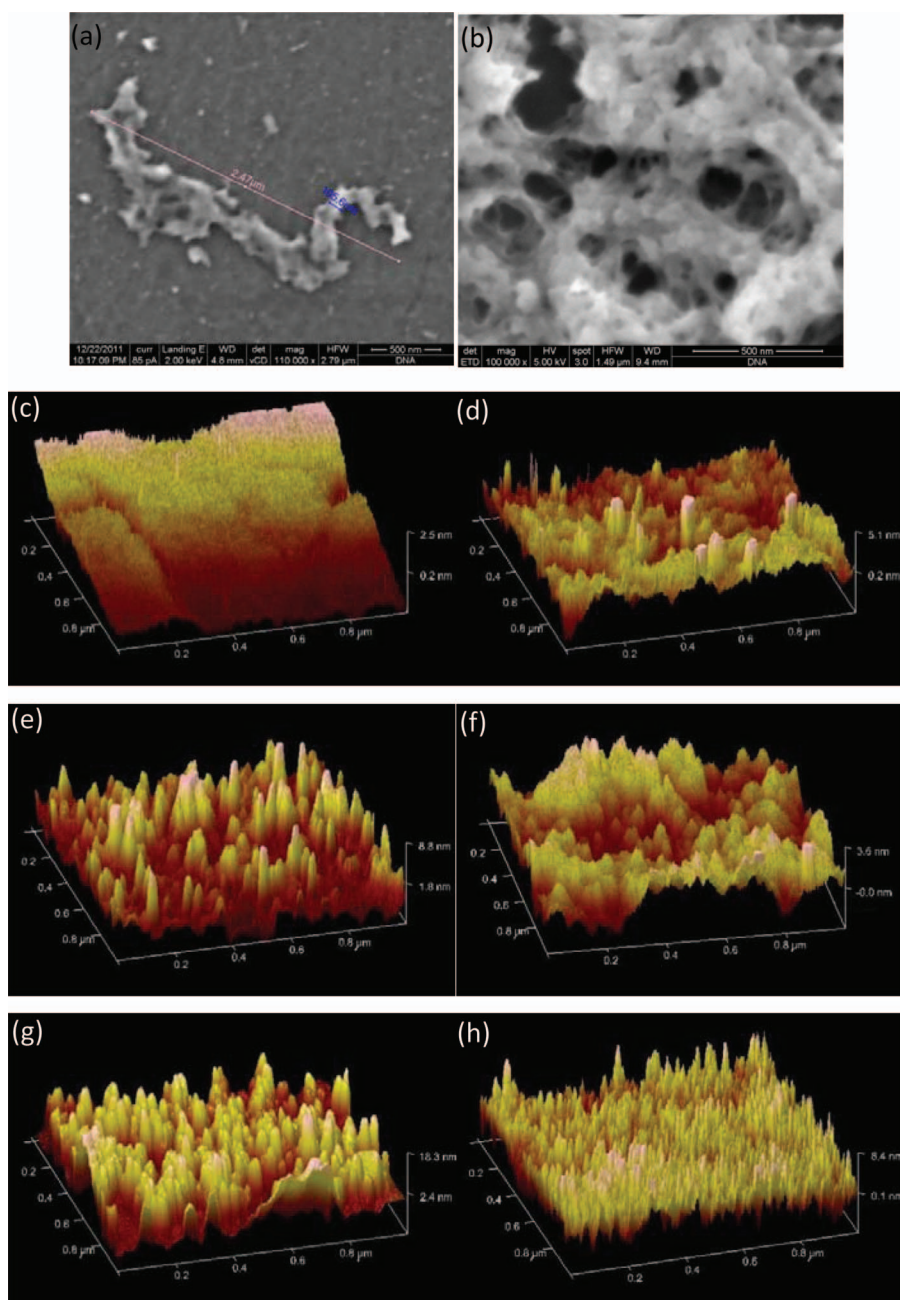

Figure 1. SEM and AFM images on GC plates: (a) SEM image of DNA aggregates. (b) SEM image of DNA-nickel aggregates. (c) AFM image of bare GC plate. (d) AFM image of 0.1M NaCl electrodeposited on GC plate. (e) AFM image of DNA aggregates. (f) AFM image of 0.5 mg/mL NiCl$_2$ electrodeposited on GC plate. (g) AFM image of DNA-nickel aggregates. (h) AFM image of DNA-nickel aggregates after 48 hr bulk electrolysis at 0.67 V in 0.1 M Methanol+0.1 M NaOH solution.

with a range from 5–25 nm. All of the aggregates have a diameter between 40–50 nm. The DNA-nickel aggregates are slightly larger than DNA aggregates, probably due to the easier crosslinking of DNA strands and the shielding of negative charges of phosphate groups. These unique DNA aggregate structures may result from the high voltage (1.8 V) applied during the electrodeposition, the hydrophobic and relative rough feature of glassy carbon surfaces, and the high concentration of DNA solution used, as discussed in the Supporting Information.[11] To date, it has been unclear what these effects may have on electrocatalysis.

XPS analysis was performed on the DNA and DNA-nickel aggregate samples. The results are shown in the Supporting Information with a thorough discussion.[11] In summary, the bases in DNA and DNA-nickel aggregates were oxidized during electrodeposition. The atomic percentages show there is approximately 1 nickel atom per 5 DNA bases in the DNA-nickel aggregates and the nickel ions interact with water, imine, carbonyl (carboxylate groups if they exist) and phosphate groups in DNA-nickel aggregates to form complex coordinated nanomaterials. DNA-nickel aggregates may also have some intramolecular electron transfer properties.

The electrocatalytic properties of DNA-nickel aggregates in alkaline media were characterized with cyclic voltammetry. Figure 2 shows a representative cyclic voltammogram of the nickel control and DNA-nickel aggregate modified glassy carbon electrodes in a blank 0.1M NaOH solution. Figure 3 shows the representative cyclic voltammograms of nickel control and DNA-nickel aggregate modified glassy carbon electrodes in different fuel solutions (methanol, ethanol, glycerol, formate, formaldehyde and glucose) in 0.1M NaOH. Bare GC electrodes and DNA aggregate modified GC electrodes were also used as controls. Ni(II)/Ni(III) redox peaks were observed with the nickel (0.370 V and 0.439 V) and the DNA-nickel aggregate modified electrodes (0.341 V and 0.420 V), as well as the irreversible fuel oxidation peaks. The peak positions of fuel oxidation, Ni(II) and Ni(III) and the current of fuel oxidation are summarized in Table I. Similar to other nickel complex electrocatalysts, nickel was first oxidized to Ni(III) in alkaline solution, and then the Ni(III) oxidized the fuels irreversibly. In the cathodic scan, both freshly chemisorbed substrate and residual adsorbed carbonaceous species were oxidized,[2] and then Ni(III) was reduced to Ni(II). The oxidation peaks of glycerol and glucose are much broader than methanol and ethanol, and they have much higher peak currents, especially the glucose, suggesting either more electrons were produced during oxidation of glycerol and glucose or a faster catalytic reaction with these fuels. The "dip" during the cathodic scan is not due to breaking down or serious morphological changes of the
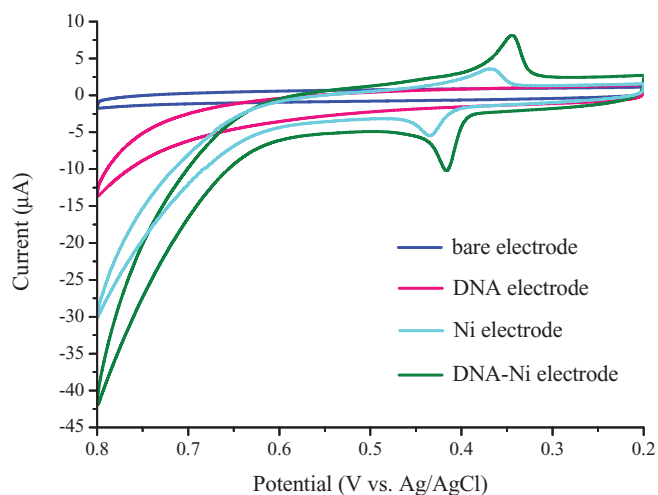
Figure 2. Cyclic voltammograms on DNA-nickel electrocatalyst at a scan rate of 0.05 V/s in a degassed solution of 0.1 M NaOH.

electrocatalyst during the cathodic scan for the DNA-nickel aggregates, since the voltammograms are quite stable during multiple scans (>100 scans). Wei et al. contributed this "dip" to the reduction of strongly adsorbed OH⁻ making available sites for methanol oxidation to happen again,[16] while other studies of nano-structured nickel oxide contributed this to the diffusion and convection mass transfer or the reduction of the passive film formed during anodic scan making fuel oxidation occur again during the cathodic scan.[17,18]

One of the truly interesting pieces of information observed when comparing the nickel control electrodes to the DNA-nickel aggregate modified electrodes is that the different structures formed with the DNA-nickel aggregate modified electrodes have differing selectivity for oxidation. Although, there is no statistical difference in oxidation current for nickel control electrodes and DNA-nickel aggregate electrodes for methanol, ethanol, glycerol, and glucose, there is a statistical difference at the 95% confidence level for formate and formaldehyde. A 80.1% current enhancement is observed for formate and a 51.9% current enhancement is observed from formaldehyde. The DNA-nickel aggregate increases the oxidative peak for formate and formaldehyde showing that there is a mechanistic change in

Table I. Peak positions of fuel oxidation, Ni(II) and Ni(III) and the current of fuel oxidation at scan rate 0.05 V/s. Data were averaged from triplicate electrodes. All of the fuel solutions are in 0.1 M NaOH.

Solution	Film	E_p red (V)	E_p ox (V)	Oxidation E (V)	Oxidation i (µA)
0.1 M NaOH	Ni	0.370 ± 0.013	0.439 ± 0.010	N/A	N/A
	DNA-nickel	0.341 ± 0.011	0.420 ± 0.002		
0.1 M Sodium	Ni	0.379 ± 0.001	0.446 ± 0.002	(Oxidative	19.6 ± 2
Formate	DNA-nickel	0.380 ± 0.002	0.448 ± 0.002	i – enhancement)	35.3 ± 7
0.1 M	Ni	[a]	[a]	0.686 ± 0.011	466 ± 5
Formaldehyde	DNA-nickel			0.770 ± 0.013	708 ± 1
0.1 M Methanol	Ni	0.378 ± 0.014	0.442 ± 0.015	0.594 ± 0.015	8.78 ± 5.09
	DNA-nickel	0.345 ± 0.006	0.418 ± 0.001	0.574 ± 0.012	10.98 ± 1.84
0.1 M Ethanol	Ni	0.374 ± 0.008	0.442 ± 0.011	0.408 ± 0.014	39.23 ± 4.86
	DNA-nickel	0.349 ± 0.005	0.426 ± 0.002	0.388 ± 0.005	46.24 ± 9.33
0.025 M	Ni	0.348 ± 0.007	0.454 ± 0.007	0.608 ± 0.015	34.28 ± 10.15
Glycerol	DNA-nickel	0.349 ± 0.005	0.437 ± 0.006	0.579 ± 0.016	32.04 ± 10.14
0.1 M Glucose	Ni	[a]	[a]	0.566 ± 0.021	85.13 ± 27.71
	DNA-nickel			0.556 ± 0.008	74.22 ± 8.08

[a]The Ni(II) and Ni(III) redox peaks are not defined in the formaldehyde and glucose cyclic voltammograms, because the formaldehyde and glucose oxidation peaks are too broad.
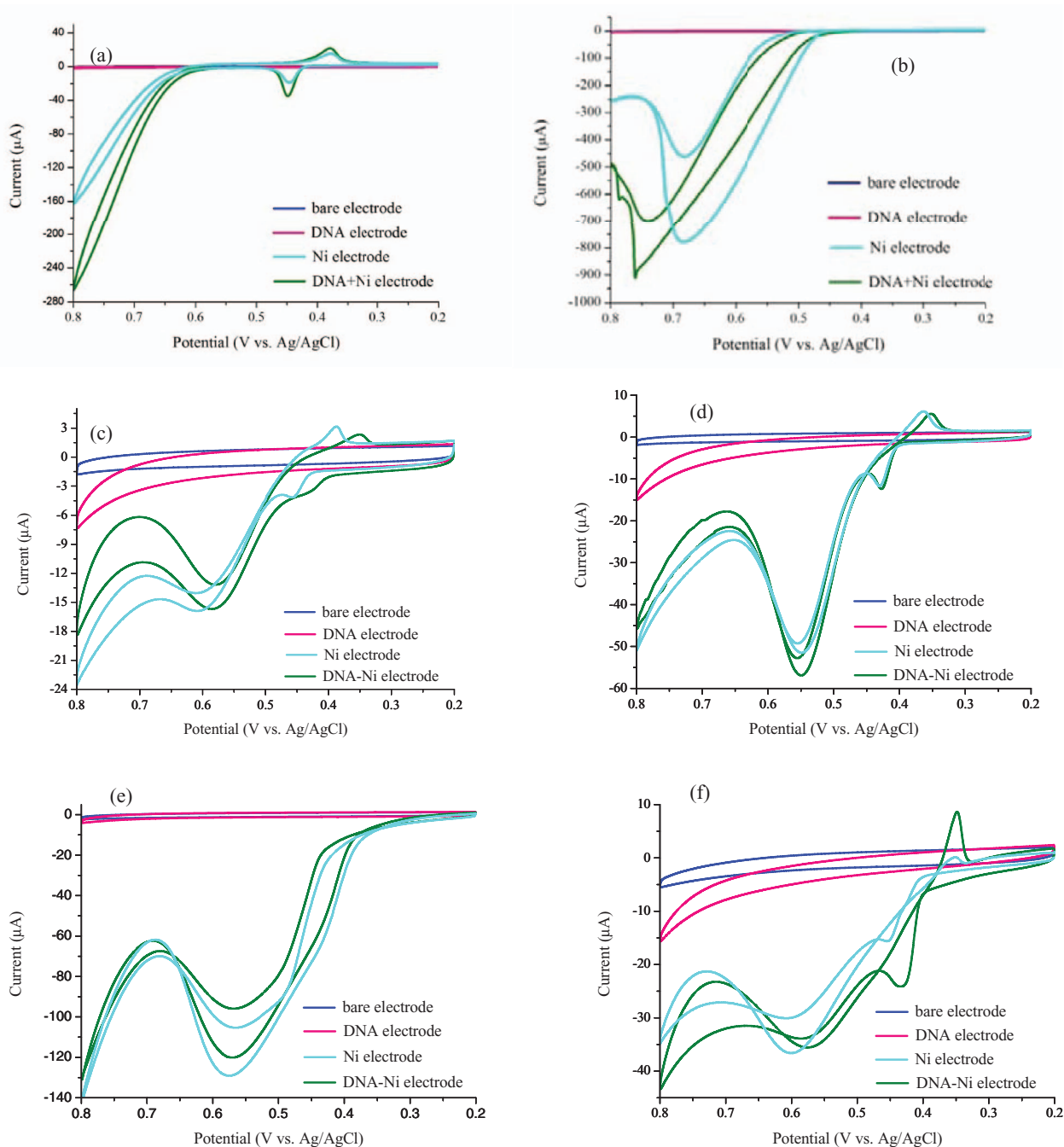
Figure 3. Cyclic voltammograms on DNA-nickel electrocatalyst at a scan rate of 0.05 V/s in degassed solutions: (a) 0.1 M NaOH and 0.1 M sodium formate, (b) 0.1 M NaOH and 0.1M formaldehyde, (c) 0.1 M NaOH and 0.1 M methanol, (d) 0.1 M NaOH and 0.1 M ethanol, (e) 0.1 M NaOH and 0.025 M glycerol, (f) 0.1 M NaOH and 0.025 M glucose.

methanol, formate, and formaldehyde oxidation at these DNA-nickel aggregate electrocatalyst.

An important feature of any fuel cell or battery is its high energy density. The energy density of methanol, ethanol, glycerol and glucose fuels are 6.1, 8.0,[19] 5.0,[20] 4.4[21] kWh/kg, respectively. Although these energy densities are lower than gasoline 10.5 kWh/kg,[19] they are large compared to the energy density of typical batteries. In order to realize high energy densities, deep oxidation of the fuels is required. Bulk electrolysis with C^{13} NMR analysis of the oxidation products was used to characterize the oxidation reactions of each of the fuels tested. Table II presents the main products of each fuel. The presence of carbonate in the products indicates that the DNA-nickel aggregates

can deeply oxidize all of the fuels except ethanol, probably due to the fact that acetate is a very thermodynamically stable intermediate product[22] while no such stable intermediate product exists during methanol oxidation.[23]

The deep oxidation of glycerol and glucose to carbon dioxide shows the oxidation catalyzed by DNA-nickel aggregates in alkaline media can even break the carbon-carbon bond, which many precious metal-based catalysts cannot.[24] It also appears that additional hydroxyl functional groups improve deep oxidation. In methanol, the carbonate product appears after 24 to 48 hours, while in glycerol and glucose the carbonate product appears after 2 to 24 hours. This is consistent with other inorganic catalysts. For instance, the oxidation of various

Table II. Product distributions of the oxidations of methanol, ethanol, glycerol and glucose.

Fuels	Main products[a]		
0.1M Methanol	formate	carbonate	formaldehyde
0.1M Ethanol	acetate		
0.025M Glycerol	formate	carbonate	
0.025M Glucose	formate	carbonate	oxalate

[a]In ^{13}C NMR, formate peak is at 171.2 ppm, carbonate peak is at 168.4 ppm, formaldehyde peak is at 82.7 ppm, and oxalate peak is at 173.5 ppm.[11]

carbohydrates at copper electrodes also indicated the need for the presence of at least two hydroxyl group for facile oxidation, and preferably more.[25] All these attributes make DNA-nickel aggregates intriguing for use in various alcohol and glucose fuel cells.

Conclusions

DNA-nickel aggregates were immobilized onto GC electrode surfaces as nanoparticles, which were characterized by AFM, SEM, and XPS. The DNA-nickel aggregates have higher density of nickel metal centers that have catalytic activities for oxidizing methanol, ethanol, glycerol and glucose. Methanol, glycerol and glucose can be completely or deeply oxidized by DNA-nickel aggregates, as shown by the presence of carbon dioxide/carbonate groups in the fuel solution. This phenomenon makes DNA-nickel aggregates a candidate as fuel cell electrocatalysts. Although current research has focused on the structure/function relationships of the catalysts, future research will focus on developing techniques for increasing the stability and the catalyst loading on electrode surfaces to increase current density, which is necessary for their use as fuel cell electrocatalysts. The DNA-nickel aggregate electrodes have similar stability to any nickel electrodeposited electrodes in alkaline media.

Supporting Information

Experimental procedures and results and discussion of X-ray photoelectron spectroscopy experiments.

References

1. T. S. Zhao, *Micro Fuel Cells: Principles and Applications*, Elsevier Burlington, MA, USA; San Diego, California, USA; London WC1X 8RR, UK (2009).
2. V. Bambagioni, C. Bianchini, A. Marchionni, J. Filippi, F. Vizza, J. Teddy, P. Serp, and M. Zhiani, *Journal of Power Sources*, **190**, 241 (2009).
3. S. S. A. Syed-Hassan, W. J. Lee, and C.-Z. Li, *Chemical Engineering Journal*, **147**, 307 (2009).
4. J. C. Harfield, K. E. Toghill, C. Batchelor-McAuley, C. Downing, and R. G. Compton, *Electroanalysis*, **23**, 931 (2011).
5. A. N. Golikand, M. Asgari, M. G. Maragheh, and S. Shahrokhian, *Journal of Electroanalytical Chemistry*, **588**, 155 (2006).
6. M. Revenga-Parra, T. García, E. Lorenzo, and F. Pariente, *Sensors and Actuators B: Chemical*, **130**, 730 (2008).
7. R. Ojani, J. Raoof, and S. Zavvarmahalleh, *Electrochimica Acta*, **53**, 2402 (2008).
8. Y. Liu, W. Wei, X. Liu, X. Zeng, Y. Li, and S. Luo, *Microchimica Acta*, **168**, 135 (2010).
9. K. Schlosser and Y. Li, *Chemistry & biology*, **16**, 311 (2009).
10. H. Li, J. D. Carter, and T. H. LaBean, *Materials Today*, **12**, 24 (2009).
11. See supplementary material at http://dx.doi.org/10.1149/2.002302eel.html.
12. A. M. Chiorcea-Paquim, O. Corduneanu, S. C. B. Oliveira, V. C. Diculescu, and A. M. Oliveira-Brett, *Electrochimica Acta*, **54**, 1978 (2009).
13. V. Andrushchenko, Z. Leonenko, D. Cramb, H. van de Sande, and H. Wieser, *Biopolymers*, **61**, 243 (2002).
14. X. Lin, X. Jiang, and L. Lu, *Biosensors & bioelectronics*, **20**, 1709 (2005).
15. K. Rippe, N. Mücke, and J. Langowski, *Nucleic acids research*, **25**, 1736 (1997).
16. Y. Liu, W. Wei, X. Zeng, and X. Liu, *Catalysis Communications*, **11**, 884 (2010).
17. W. Huang, Z. Li, Y. Peng, and Z. Niu, *Chem Commun (Camb)*, 1380 (2004).
18. N. Spinner and W. E. Mustain, *Electrochimica Acta*, **56**, 5656 (2011).
19. M. T. M. Koper, *Fuel Cell Catalysis: A Surface Science Approach*, John Wiley & Sons, Inc., Hoboken, New Jersey (2009).
20. J. F. Gomes and G. Tremiliosi-Filho, *Electrocatalysis*, **2**, 96 (2011).
21. N. Fujiwara, S.-i. Yamazaki, Z. Siroma, T. Ioroi, H. Senoh, and K. Yasuda, *Electrochemistry Communications*, **11**, 390 (2009).
22. H.-F. Wang and Z.-P. Liu, *Journal of the American Chemical Society*, **130**, 10996 (2008).
23. S. K. Desai, M. Neurock, and K. Kourtakis, *The Journal of Physical Chemistry B*, **106**, 2559 (2002).
24. R. L. Arechederra and S. D. Minteer, *Fuel Cells*, **9**, 63 (2009).
25. M. Z. Luo and R. P. Baldwin, *Journal of Electroanalytical Chemistry*, **387**, 87 (1995).